Electronic Supplementary Information

Modulating the Electrical Conductivity of a Graphene Oxide-coated 3D Framework for Guiding Bottom-up Lithium Growth

Kwang Hyun Park,[a,‡] Dong Woo Kang,[b,c,‡] Jun-Woo Park,[b] Jeong-Hee Choi,[b] Soon-Jik Hong,[a] Sung Ho Song,[a] Sang-Min Lee,[b] Janghyuk Moon[d,*] and Byung Gon Kim[b,*]

[a] *Division of Advanced Materials Engineering, Kongju National University, 1223-24, Cheonan-daero, Seobuk-gu, Cheonan-si, Chungcheongnam-do 31080, Republic of Korea*

[b] *Next Generation Battery Research Center, Korea Electrotechnology Research Institute (KERI), 12, Jeongiui-gil, Seongsan-gu, Changwon-si, Gyeongsangnam-do 51543, Republic of Korea. E-mail: byunggonkim@keri.re.kr*

[c] *School of Materials Science and Engineering, Pusan National University, 2, Busandaehak-ro 63beon-gil, Geumjeong-gu, Busan 46241, Republic of Korea*

[d] *School of Energy Systems Engineering, Chung-Ang University, Heukseok-ro, Dongjak-gu, Seoul 06974, Republic of Korea. E-mail: jhmoon84@cau.ac.kr*

‡ These authors contributed equally to this work.

Fig. S1. Dispersion characteristics of GO at various IPA–DI water mixture ratios (e.g., 2 (IPA) : 8 (DI water) ~ 8 : 2).

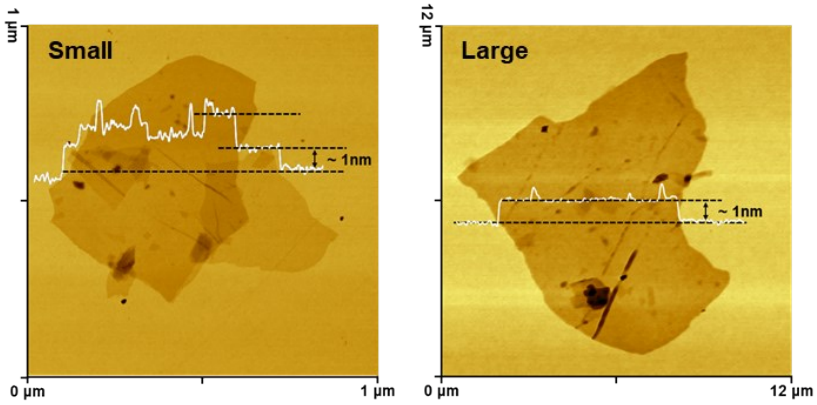

Fig. S2. AFM images of small (SGO) and large GO (LGO) flakes with thicknesses of ~ 1 nm.

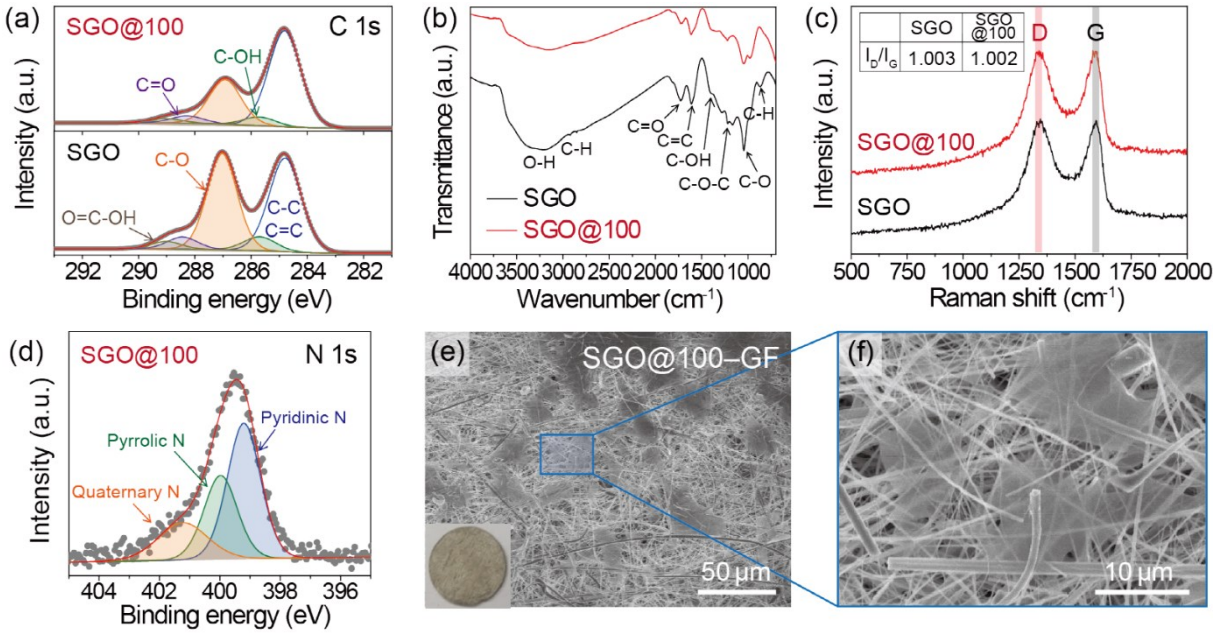

Fig. S3. (a) C 1s XPS, (b) FT-IR, (c) Raman, and (d) N 1s XPS spectra of SGO and SGO@100. (e) SEM and digital photograph images (inset) of SGO–GF used in this study. (f) A magnified SEM image of region enclosed by the blue box in panel (e).

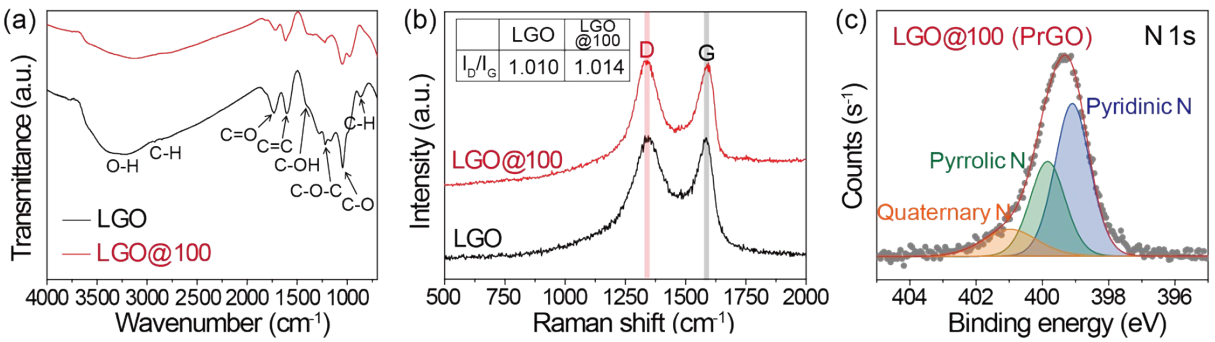

Fig. S4. (a) FT-IR, (b) Raman, and (c) N 1s XPS spectra of LGO and LGO@100.

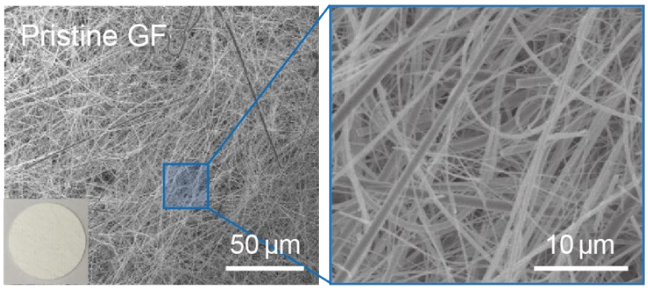

Fig. S5. (Left) SEM and digital photographic (inset) images of the pristine GF used in this study. (Right) An SEM image magnified from the blue box.

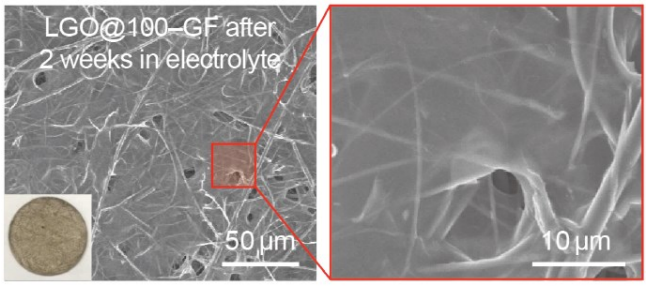

Fig. S6. (Left) SEM and digital photographic (inset) images of LGO@100–GF after immersion test in the electrolyte for two weeks. (Right) An SEM image magnified from the left red box. Morphological changes were not observed when compared to the pristine sample.

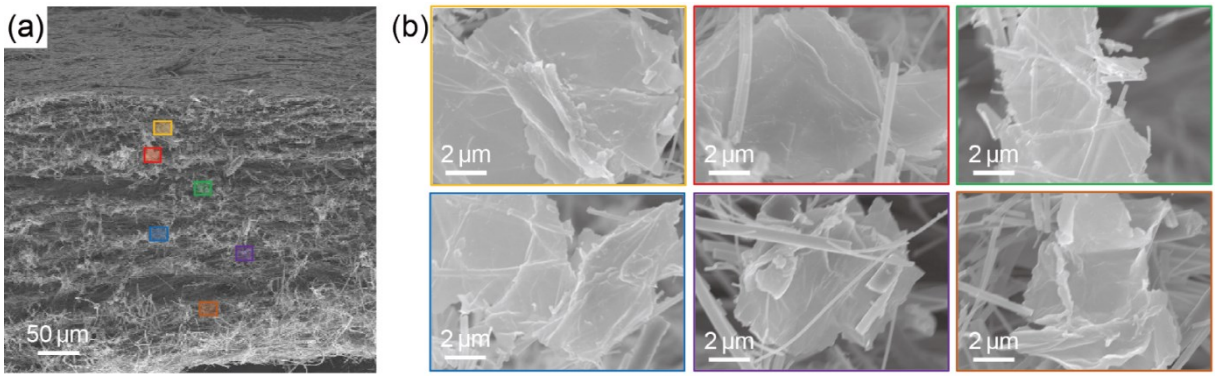

Fig. S7. Cross-sectional SEM images of the LGO@100–GF framework at (a) low- and (b) high-magnifications. The images in the colored square in (b) were acquired from the same-colored squares in (a). Some small particles corresponding to the small-size range in the size distribution shown in Fig. 1c appear to be observed inside the LGO@100–GF framework.

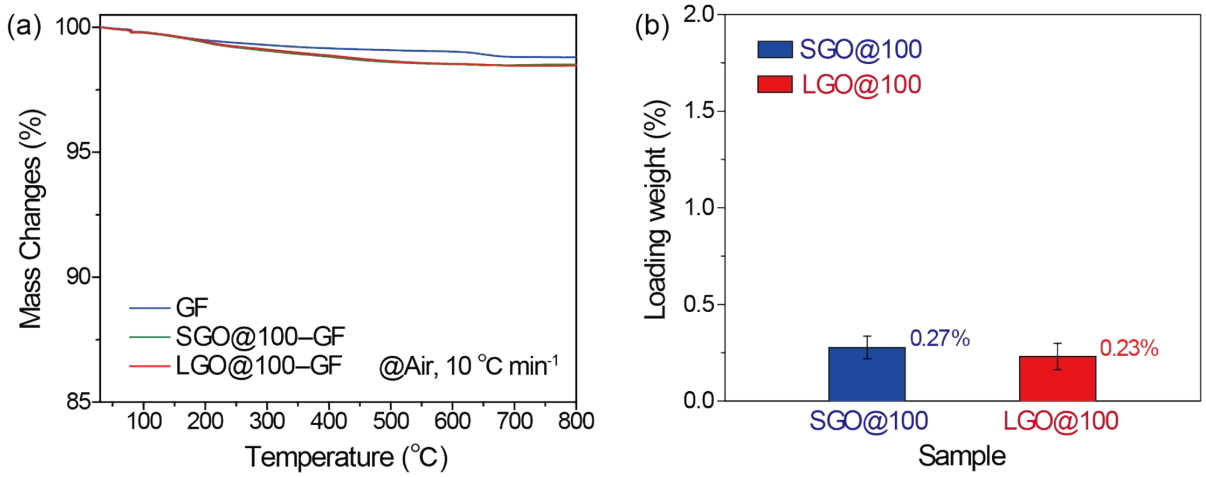

Fig. S8. (a) TGA profiles of GF, SGO@100–GF, and LGO@100–GF in air. (b) Loading weight of SGO@100 and LGO@100 in SGO@100–GF and LGO@100–GF frameworks, respectively. The average loading weight and standard deviation were obtained from 10 TGA analyses.

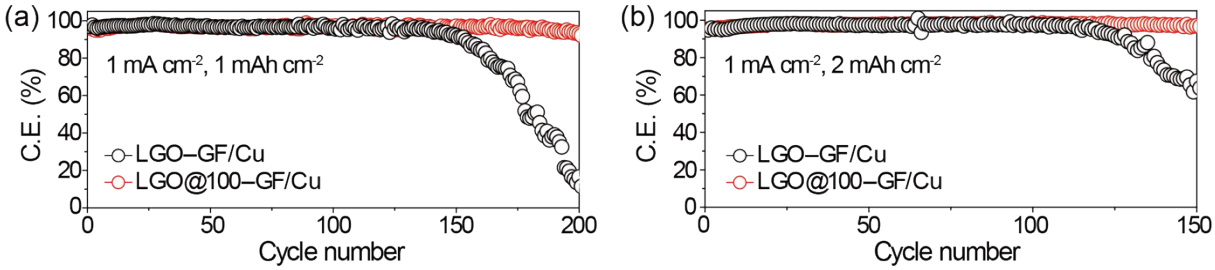

Fig. S9. CEs of LGO–GF/Cu and LGO@100–GF/Cu at a current density of 1 mA cm^{-2} with Li plating/stripping capacities of: (a) 1 mAh cm^{-2} and (b) 2 mAh cm^{-2}.

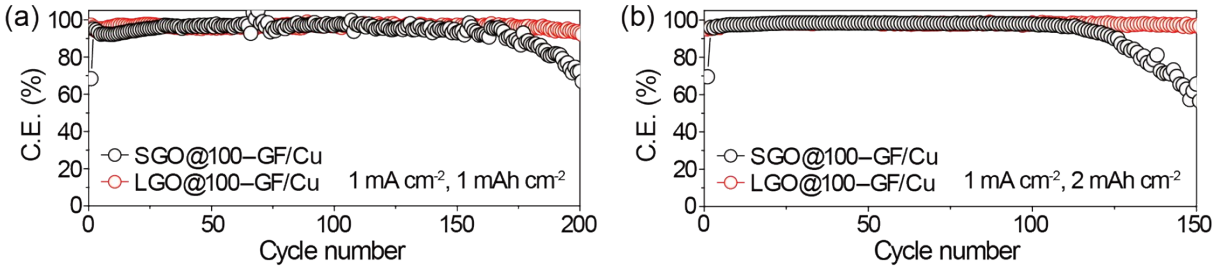

Fig. S10. CEs of SGO@100–GF/Cu and LGO@100–GF/Cu at a current density of 1 mA cm^{-2} with Li plating/stripping capacities of: (a) 1 mAh cm^{-2} and (b) 2 mAh cm^{-2}.

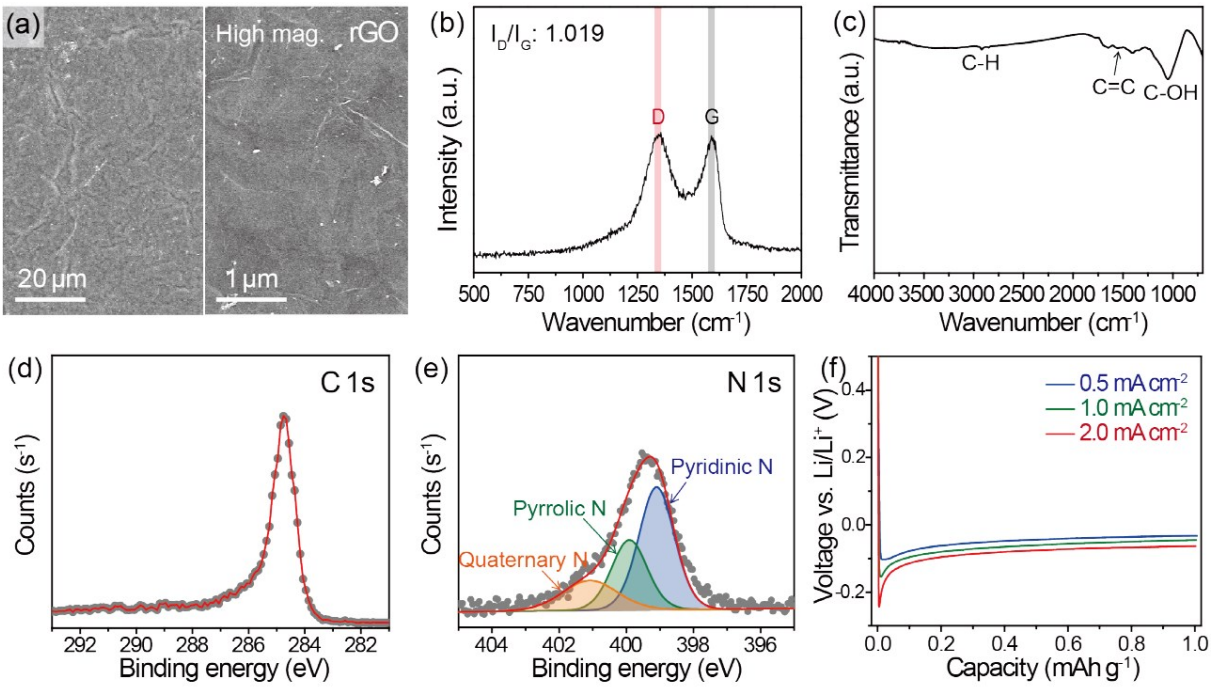

Fig. S11. The rGO electrode for electrochemical characterization. (a) SEM images and (b) Raman, (c) FT-IR, (d) C 1s, and (e) N 1s XPS spectra of rGO. (f) Voltage profiles of the rGO sample during Li plating when measured at a capacity of 1 mAh cm^{-2} with different current densities of 0.5, 1.0, and 2.0 mA cm^{-2}.

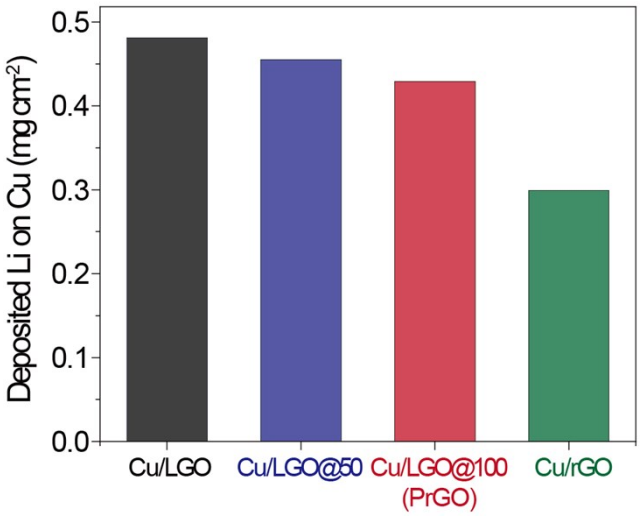

Fig. S12. The deposited Li weight on Cu in various half-moon shaped Cu/LGO, Cu/LGO@50, Cu/LGO@100, and Cu/rGO electrodes after Li plating at 1 mA cm^{-2} and 1mAh cm^{-2}. When the 1 mAh cm^{-2} of Li is totally electrodeposited on Cu, the weight should increase by 0.5181 mg cm^{-2}.

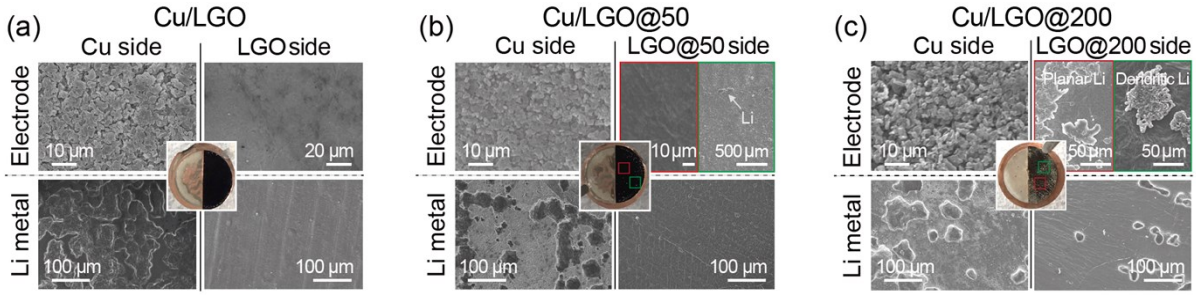

Fig. S13. Digital photographs (center inset) and SEM images from various viewpoints of half-moon-shaped (a) Cu/LGO, (b) Cu/LGO@50, and (c) Cu/LGO@200 electrodes after Li plating at a current density of 1mA cm^{-2} with a fixed capacity of 1mAh cm^{-2}.

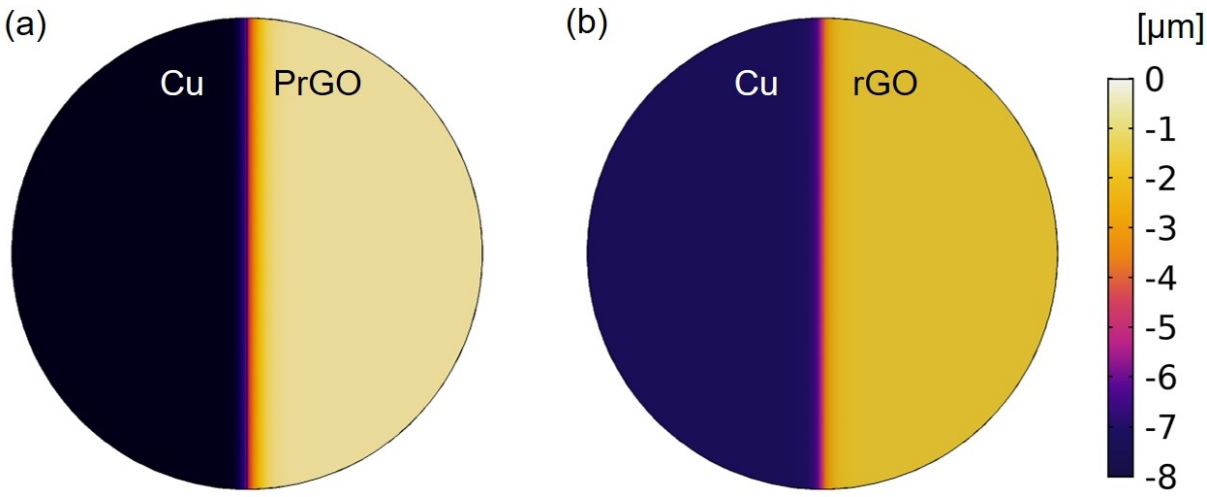

Fig. S14. Simulation results of Li stripping behavior on a Li reference/counter electrode in a half-moon-shaped Cu/PrGO cell: Li metal surfaces of (a) Cu/PrGO and (b) Cu/rGO cells at a current density of 1 mA cm^{-2} with a fixed capacity of 1 mAh cm^{-2}. Negative values correspond to the thickness of stripped Li.

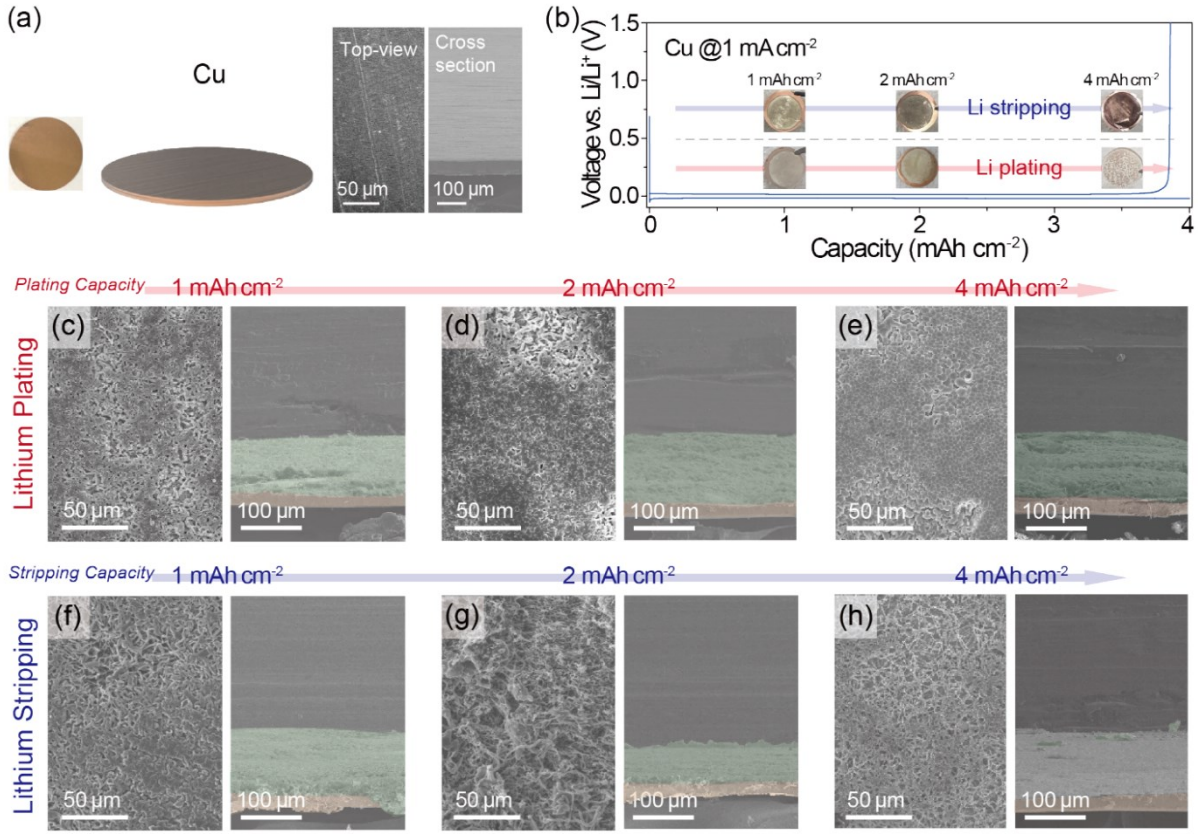

Fig. S15. (a) Digital photograph and SEM images of the pristine Cu electrode. (b) Second voltage profile of the Cu cell at 1 mA cm^{-2} with a capacity of 4 mAh cm^{-2}. (Insets) Digital photographs of the Cu electrode at different Li plating and stripping capacities. (c–h) Top-view and cross-sectional SEM images of the Cu electrode obtained at fixed Li plating/stripping capacities of 1, 2, and 4 mAh cm^{-2} in (b). The pale green color corresponds to metallic Li.

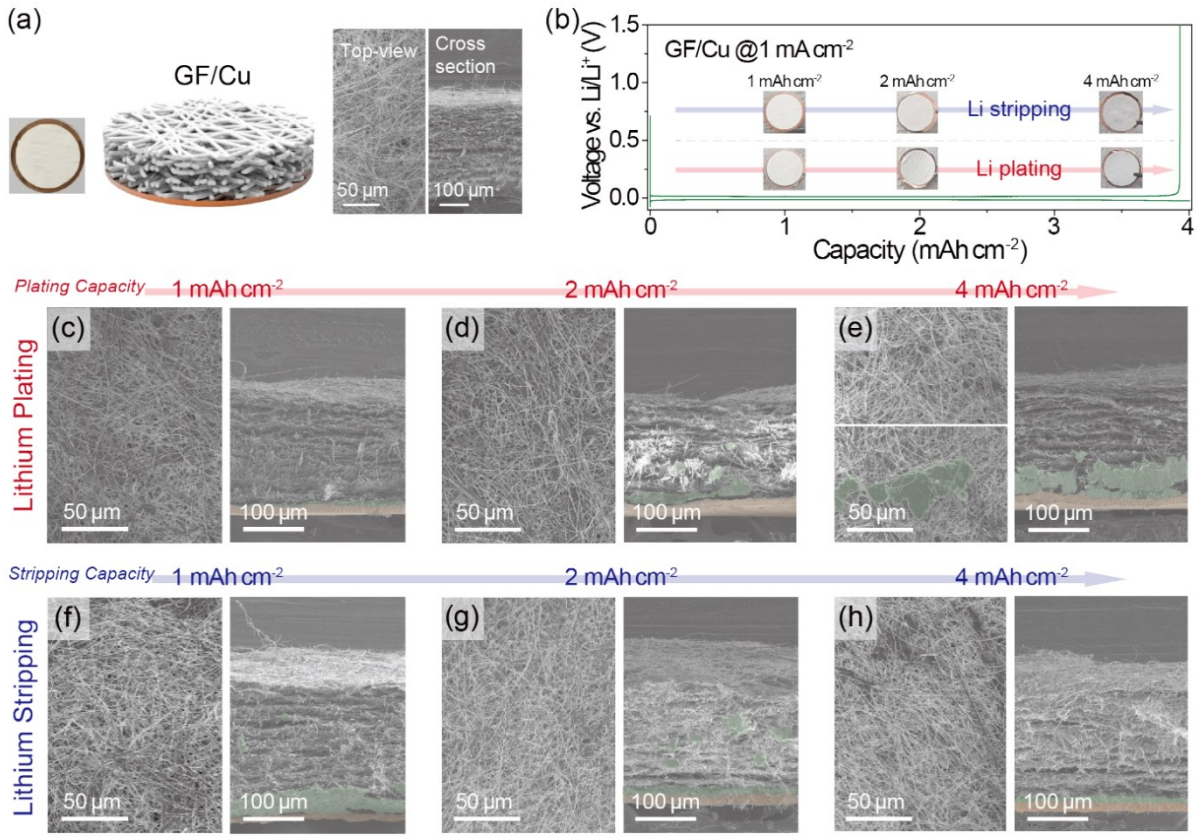

Fig. S16. (a) Digital photograph and SEM images of the pristine GF/Cu electrode. (b) Second voltage profile of the GF/Cu cell at 1 mA cm^{-2} with a capacity of 4 mAh cm^{-2}. (Insets) Digital photographs of the GF/Cu electrode at different Li plating and stripping capacities. (c–h) Top-view and cross-sectional SEM images of the GF/Cu electrode obtained at fixed Li plating/stripping capacities of 1, 2, and 4 mAh cm^{-2} in (b). The pale green color corresponds to metallic Li.

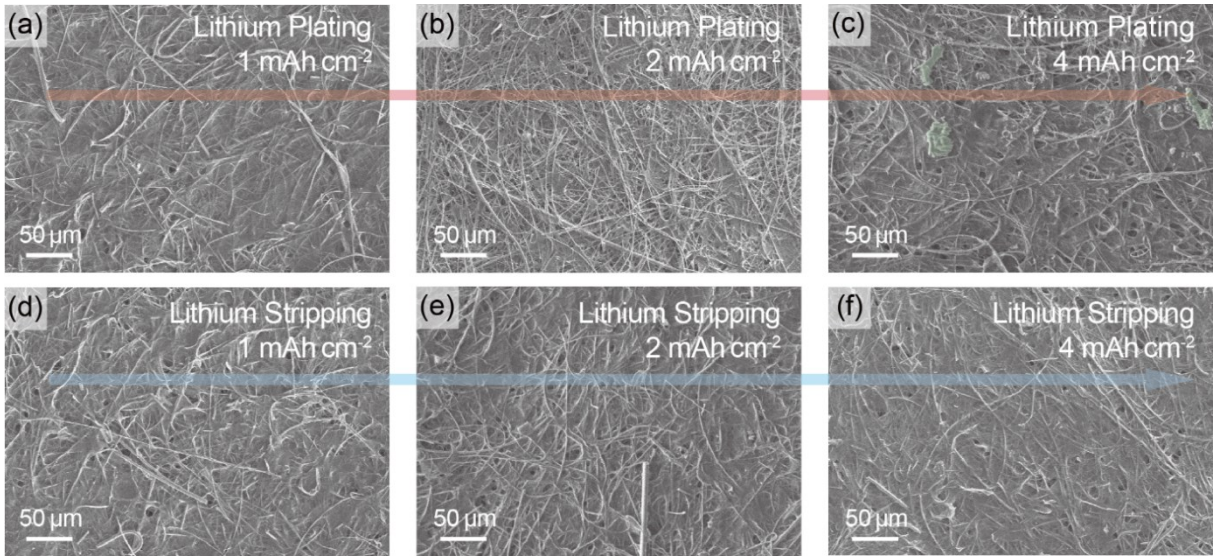

Fig. S17. Low-magnification top-view SEM images of the PrGO–GF/Cu electrode during the Li plating/stripping processes shown in Fig. 3. The pale green color corresponds to metallic Li.

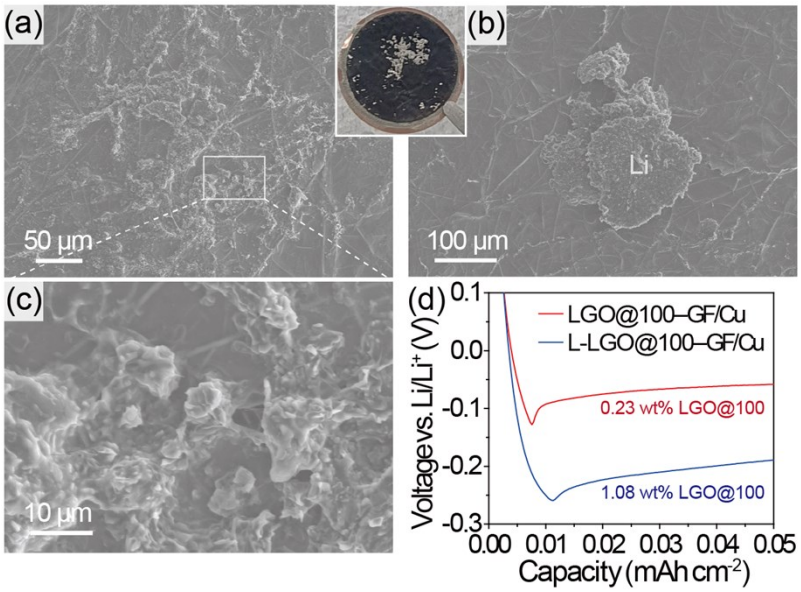

Fig. S18. (a-c) Top-view SEM images of large amount (L)-LGO@100–GF/Cu electrode after Li plating at 1 mA cm^{-2} and 4 mAh cm^{-2}. (Inset between a and b) A digital photograph of the L-LGO@100–GF/Cu electrode. (d) Li plating potentials of the LGO@100(PrGO)–GF/Cu and L-LGO@100–GF/Cu electrodes during the initial Li plating stage at a current density of 1 mA cm^{-2}.

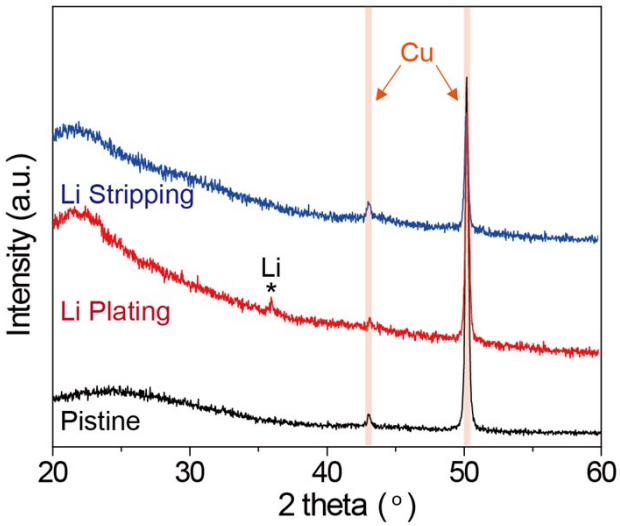

Fig. S19. XRD patterns of the PrGO–GF/Cu electrodes after the 1st Li plating and stripping processes shown in Fig. 3.

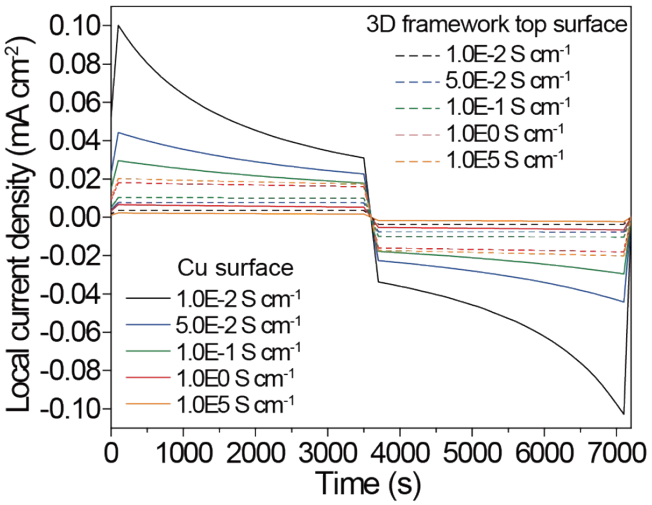

Fig. S20. Time evolutions of local current densities on the (dashed lines) top surface of framework with various electrical conductivities, and on the (solid lines) Cu surface in the 3D host. The current density of 1 mA cm^{-2} was applied for 1 h to charge and discharge processes.

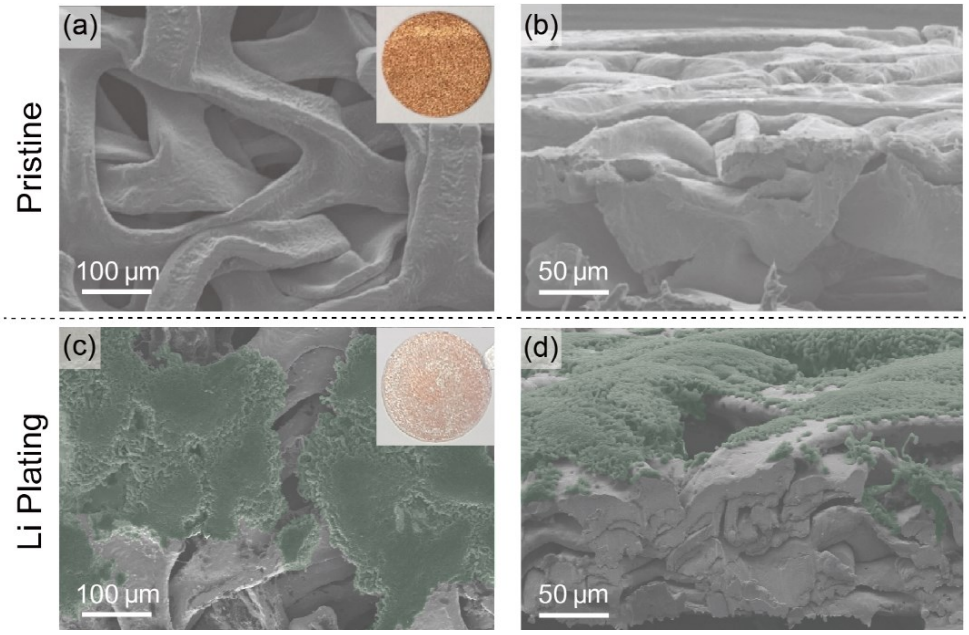

Fig. S21. Top-view and cross-sectional SEM images of 3D Cu foam (thickness: ~250 μm which is identical to that of GF) at the pristine (upper row) and after Li plating (bottom row) states (1 mA cm^{-2}, 2 mAh cm^{-2}). After the Li plating, the 3D Cu foam shows Li top plating behavior. The pale green color corresponds to metallic Li.

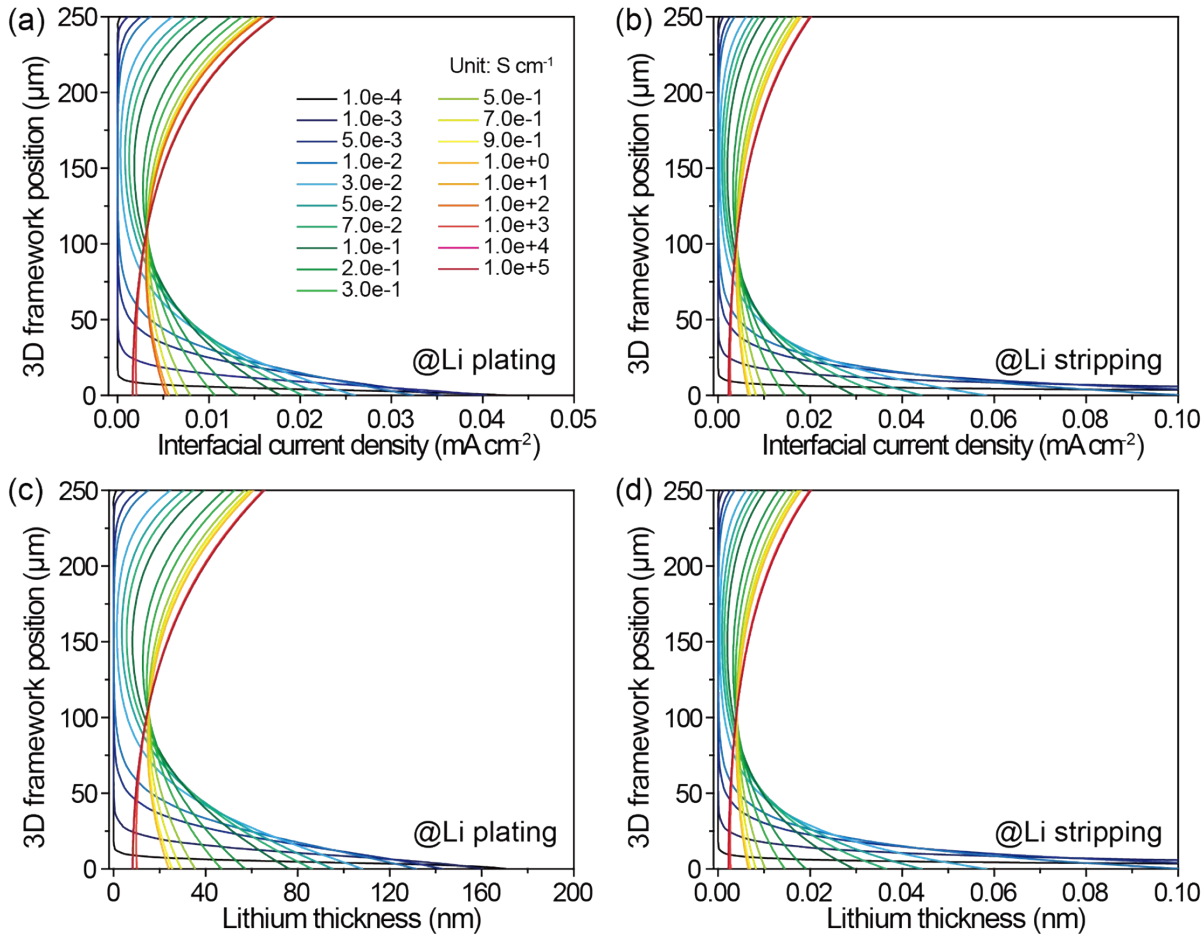

Fig. S22. Li current density in the 3D framework having various electrical conductivities along the thickness direction (top: 250 μm, bottom: 0 μm) after (a) Li plating (t = 3600 s) and (b) Li stripping (t = 7200 s) processes. Deposited and residual Li thicknesses in the framework after (c) Li plating and (d) Li stripping processes, respectively. A current density of 1 mA cm^{-2} is applied for 1 h to charge and discharge processes. The Li thickness is the average thickness of Li at the bottom region of the 3D host.

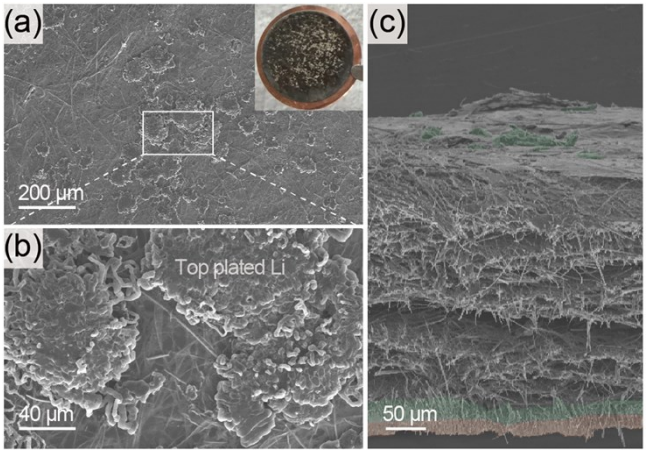

Fig. S23. (a,b) Top-view and (c) cross-sectional SEM images of LGO@200–GF/Cu electrode after Li plating at 1 mA cm^{-2} and 4 mAh cm^{-2}. (Inset in a) A digital photograph of the LGO@200–GF/Cu electrode. Because of the increased conductivity compared to that of PrGO–GF/Cu, the LGO@200–GF/Cu showed slight top plated Li on the structure apart from the deposited Li at the bottom region of the host.

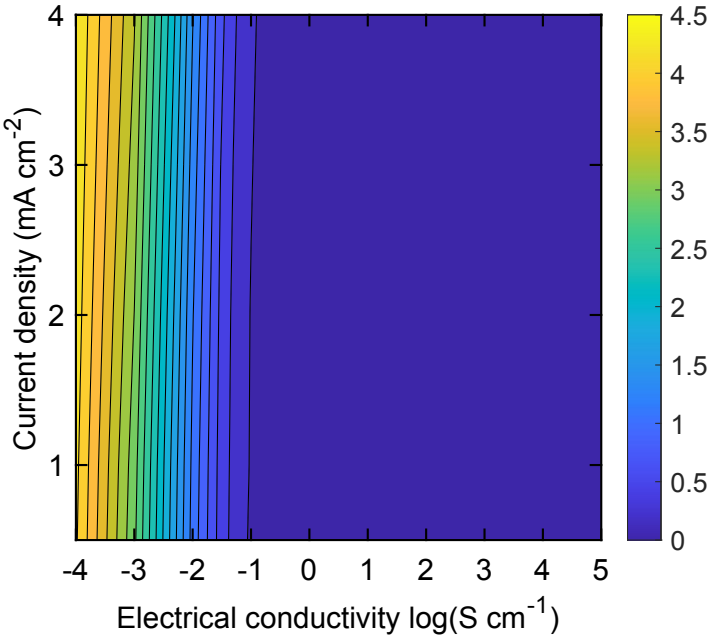

Fig. S24. Simulation results of deposited Li thickness on the Cu surface as functions of both applied current density and electrical conductivity of the 3D framework. The units of the contour map are micrometers (μm). A value of zero indicates Cu substrate with no deposited Li, and the maximum value indicates the fully deposited Li on Cu.

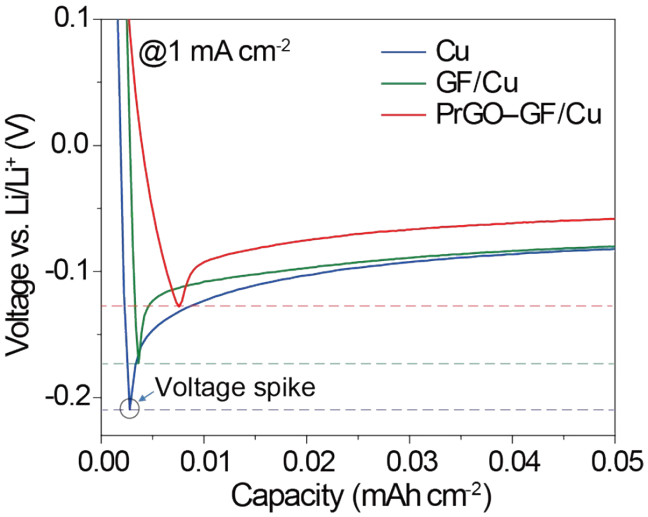

Fig. S25. Li plating potentials of the Cu, GF/Cu, and PrGO–GF/Cu electrodes during the initial Li plating stage at a current density of 1 mA cm^{-2}.

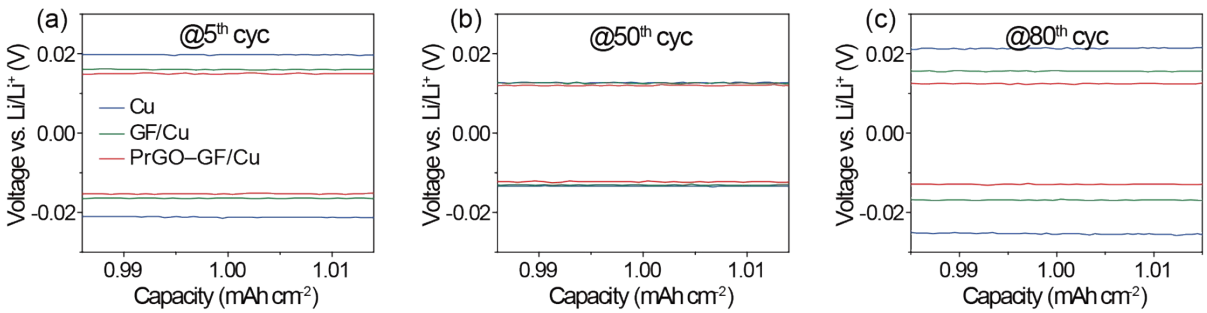

Fig. S26. Enlarged voltage profiles of the three electrodes in Fig. 5e and 5f at the (a) 5th, (b) 50th, and (c) 80th cycles.

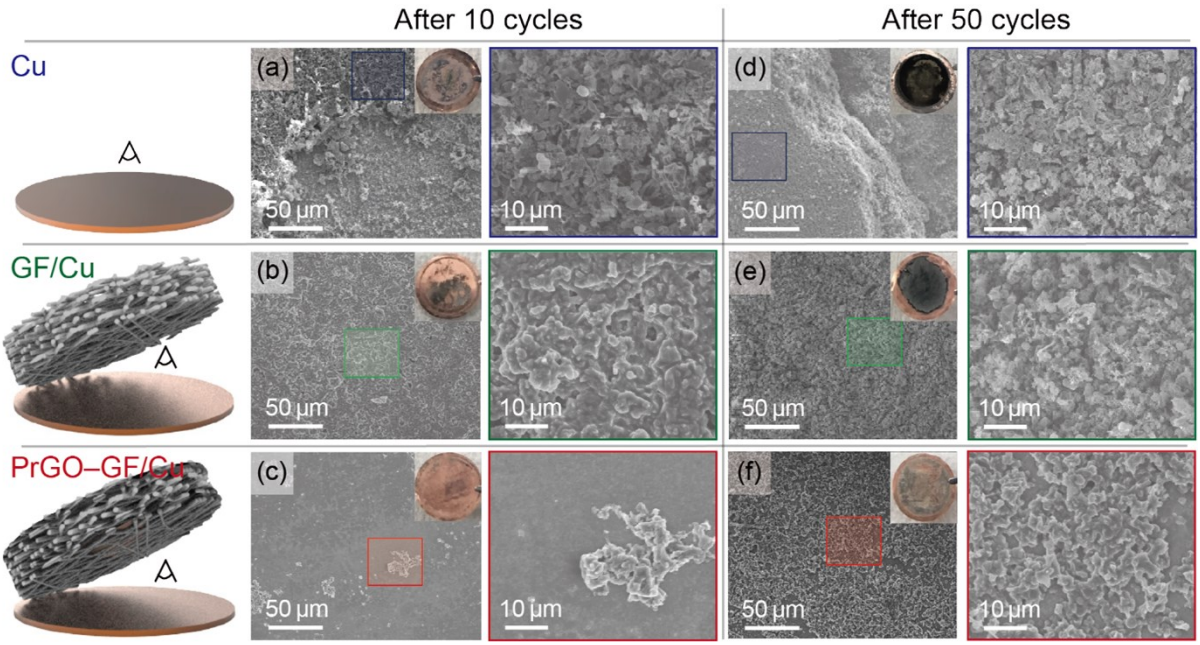

Fig. S27. SEM images of the Cu substrates of the Cu, GF/Cu, and PrGO–GF/Cu electrodes shown in Fig. 5g and 5h after 10 (a–c, left) and 50 cycles (d–f, right). Each pair of images shows (left) low- and (right) high-magnification images.

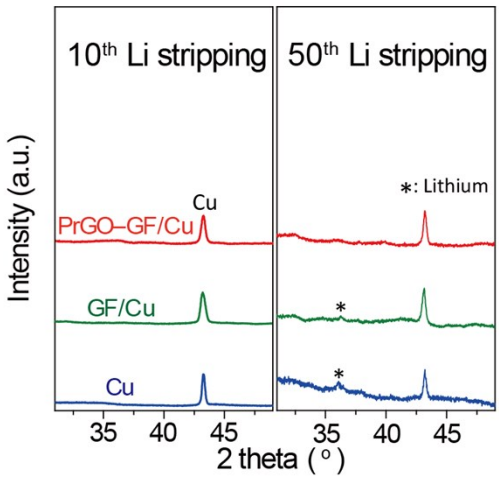

Fig. S28. XRD patterns of the Cu substrates of the Cu, GF/Cu, and PrGO–GF/Cu electrodes after the 10th and 50th Li stripping processes.

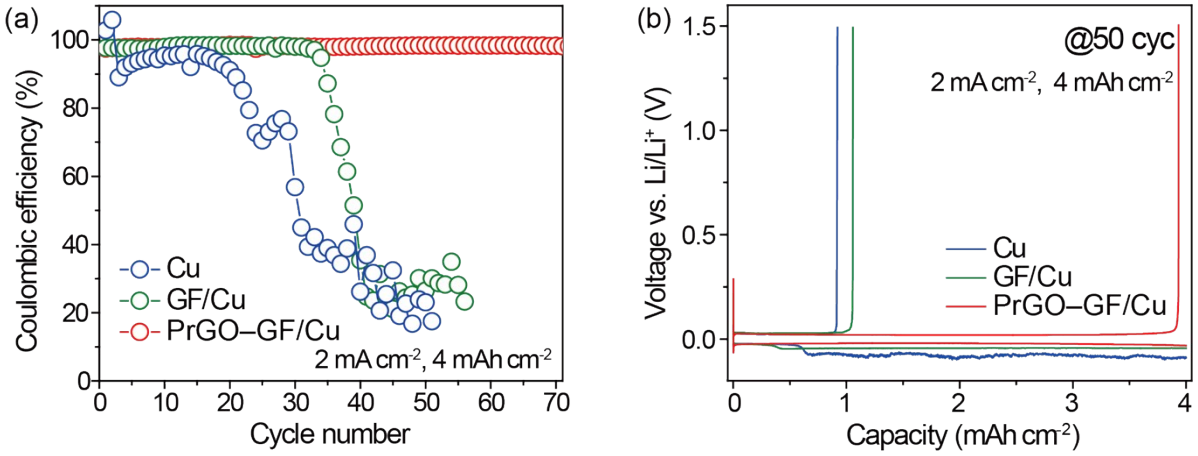

Fig. S29. (a) CEs and (b) the 50th voltage profiles of the Cu, GF/Cu, and PrGO–GF/Cu electrodes at 2 mA cm^{-2} with a fixed capacity of 4 mAh cm^{-2}.

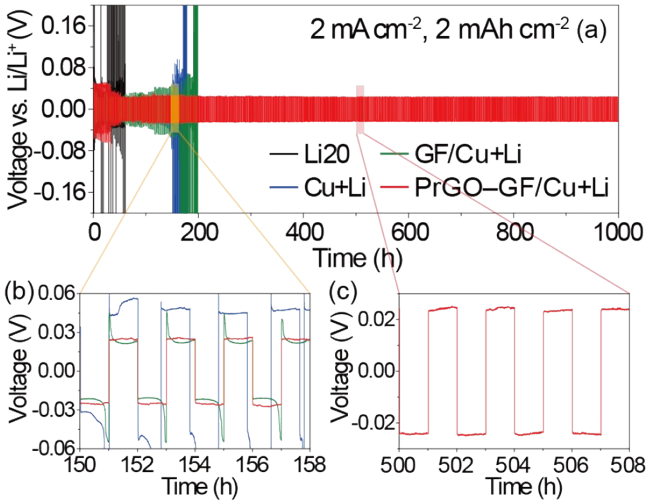

Fig. S30. Voltage profiles of symmetric cells containing Li20, Cu+Li, GF/Cu+Li, and PrGO–GF/Cu+Li electrodes at a current density of 2 mA cm^{-2} with an operating capacity of 2 mAh cm^{-2}. For this test, 4 mAh cm^{-2} Li (~20 µm) was predeposited onto Cu, GF/Cu, and PrGO–GF/Cu to form the Cu+Li, GF/Cu+Li, and PrGO–GF/Cu+Li anodes, respectively. Enlarged voltage profiles corresponding to the colored boxes in (a) from (b) cycle 75 to 79 and (c) cycle 250 to 254.

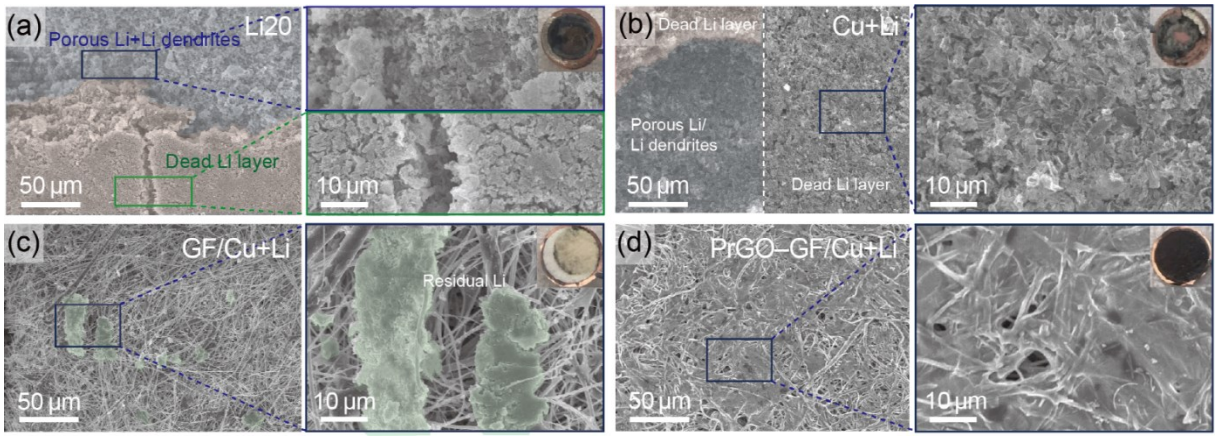

Fig. S31. SEM images of the anodes of the LFP full cells shown in Fig. 7a after 250 cycles: (a–d) top-view at low (left) and high (right) magnifications. The insets in (a–d) are digital photographs of the electrodes.

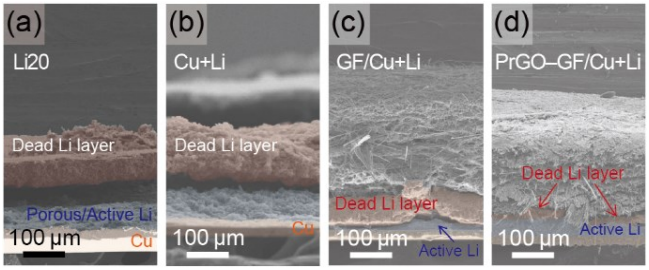

Fig. S32. Cross-sectional SEM images of the anodes of the LFP full cells shown in Fig. 7a after 250 cycles.

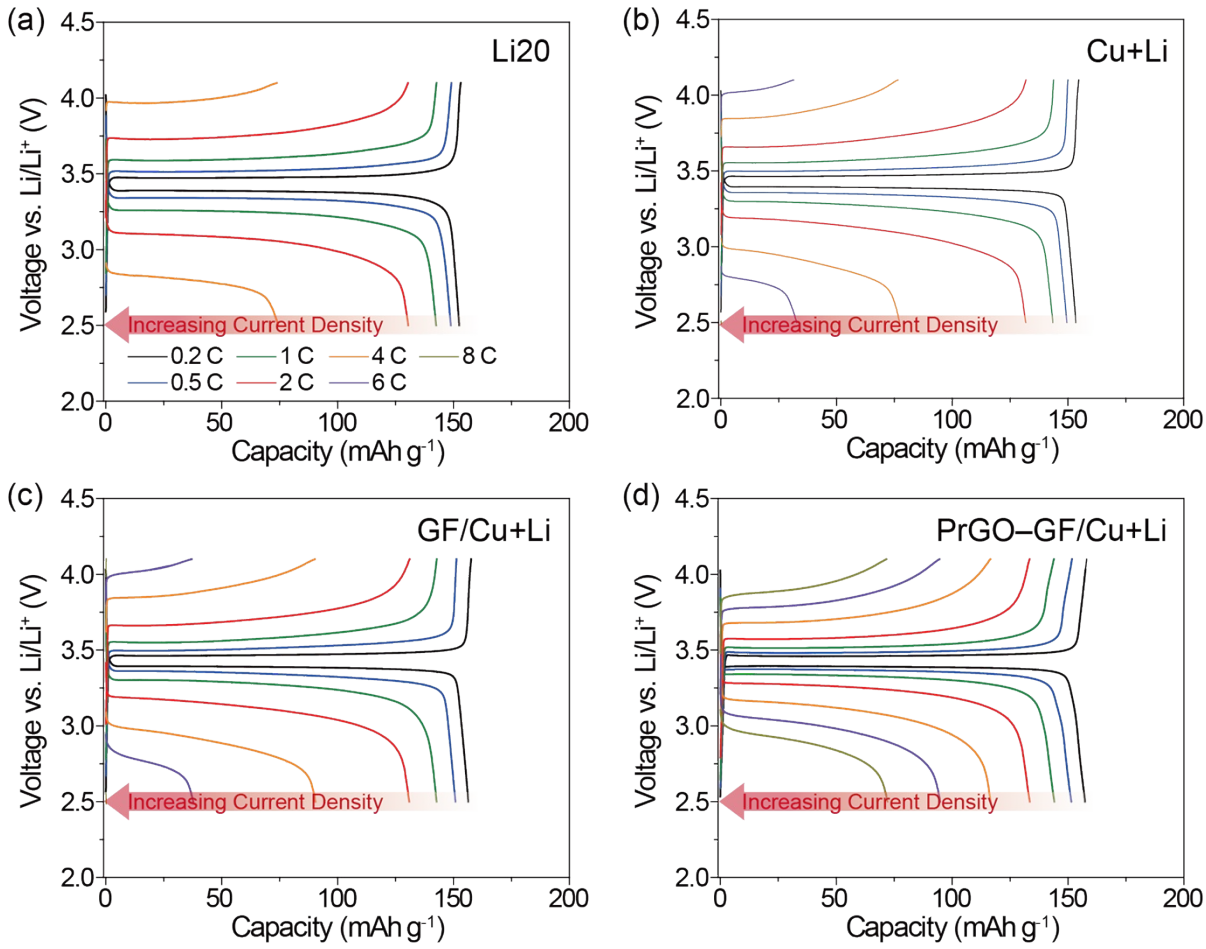

Fig. S33. Voltage profiles of cells with the Li20, Cu+Li, GF/Cu+Li, and PrGO–GF/Cu+Li electrodes at different current densities during the rate performance test shown in Fig. 6g.

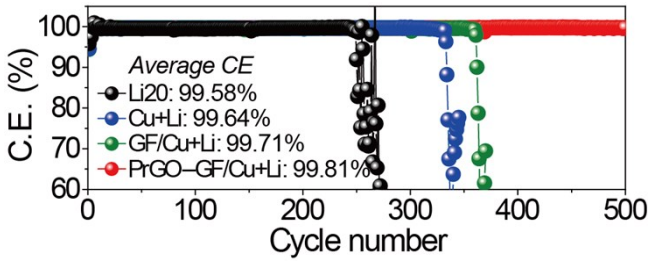

Fig. S34. Coulombic efficiencies of the LFP full cells containing Li20, Cu+Li, GF/Cu+Li, and PrGO–GF/Cu+Li electrodes shown in Fig. 7a at 0.5 C during 500 cycles. The average CEs in cycles 1 to 150 are indicated beside the legend texts.

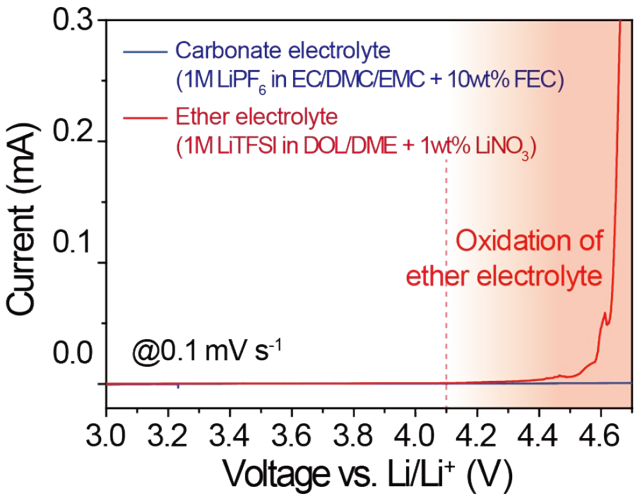

Fig. S35. Linear sweep voltammogram of the ether electrolyte used in this study and a conventional carbonate electrolyte. The red dashed line at 4.1 V indicates the upper potential cutoff of the LFP full cell test in the current study, which was used to avoid severe ether electrolyte oxidation.